

SANDIA REPORT

SAND2006-6720

Unlimited Release

Printed November 2006

Emulsions for Interfacial Filtration

Anne M. Grillet, Margaret E. Welk, Chris. J. Bourdon, Carlton F. Brooks,
Caroline A. Souza, and Joel D. Hartenberger

Prepared by
Sandia National Laboratories
Albuquerque, New Mexico 87185 and Livermore, California 94550

Sandia is a multiprogram laboratory operated by Sandia Corporation,
a Lockheed Martin Company, for the United States Department of Energy's
National Nuclear Security Administration under Contract DE-AC04-94AL85000.

Approved for public release; further dissemination unlimited.



Issued by Sandia National Laboratories, operated for the United States Department of Energy by Sandia Corporation.

NOTICE: This report was prepared as an account of work sponsored by an agency of the United States Government. Neither the United States Government, nor any agency thereof, nor any of their employees, nor any of their contractors, subcontractors, or their employees, make any warranty, express or implied, or assume any legal liability or responsibility for the accuracy, completeness, or usefulness of any information, apparatus, product, or process disclosed, or represent that its use would not infringe privately owned rights. Reference herein to any specific commercial product, process, or service by trade name, trademark, manufacturer, or otherwise, does not necessarily constitute or imply its endorsement, recommendation, or favoring by the United States Government, any agency thereof, or any of their contractors or subcontractors. The views and opinions expressed herein do not necessarily state or reflect those of the United States Government, any agency thereof, or any of their contractors.

Printed in the United States of America. This report has been reproduced directly from the best available copy.

Available to DOE and DOE contractors from
U.S. Department of Energy
Office of Scientific and Technical Information
P.O. Box 62
Oak Ridge, TN 37831

Telephone: (865) 576-8401
Facsimile: (865) 576-5728
E-Mail: reports@adonis.osti.gov
Online ordering: <http://www.osti.gov/bridge>

Available to the public from
U.S. Department of Commerce
National Technical Information Service
5285 Port Royal Rd.
Springfield, VA 22161

Telephone: (800) 553-6847
Facsimile: (703) 605-6900
E-Mail: orders@ntis.fedworld.gov
Online order: <http://www.ntis.gov/help/ordermethods.asp?loc=7-4-0#online>



Emulsions for Interfacial Filtration

Anne M. Grillet and J. Bourdon,
Department 1513, Microscale Science & Technology

Carlton F. Brooks and Joel D. Hartenberger
Department 1512, Fuels And Energy Transitions

Margaret E. Welk and Carloine A. Souza,
Department 6338, Thermal, Fluid, & Aero Experimental Sciences

Sandia National Laboratories
P.O. Box 5800
Albuquerque, New Mexico 87185-MS0834

Abstract

We have investigated a novel emulsion interfacial filter that is applicable for a wide range of materials, from nano-particles to cells and bacteria. This technology uses the interface between the two immiscible phases as the active surface area for adsorption of targeted materials. We showed that emulsion interfaces can effectively collect and trap materials from aqueous solution. We tested two aqueous systems, a bovine serum albumin (BSA) solution and coal bed methane produced water (CBMPW). Using a pendant drop technique to monitor the interfacial tension, we demonstrated that materials in both samples were adsorbed to the liquid-liquid interface, and did not readily desorb. A prototype system was built to test the emulsion interfacial filter concept. For the BSA system, a protein assay showed a progressive decrease in the residual BSA concentration as the sample was processed. Based on the initial prototype operation, we propose an improved system design.

ACKNOWLEDGMENTS

The authors gratefully acknowledge the support of the Laboratory Directed Research and Development (LDRD) program and the Seniors Council. We would also like to thank Jonathan Leonard for his help with produced water sampling and analysis, Emily Wright and Mike Hightower for providing the coal bed methane produced water samples and J. Bruce Kelley and Richard Griffith for their support and encouragement in finding applications for this technology.

CONTENTS

1. Introduction.....	7
2. Material Trapping at Emulsion Interfaces	9
3. Pendant Drop Analysis	11
4. Prototype System Analysis	21
5. Emulsion System Design	27
6. Conclusion	29
7. References.....	31
Appendix A: Chemical Analysis of Coal Bed Methane Produced Water	33
Distribution	35

FIGURES

Figure 1: Using coalescence to collapse the emulsion interfaces and concentrate the target analyte.....	8
Figure 2: Formation of emulsion, trapping of the target material at the emulsion interfaces, and coalescence of the oil phase and concentration of the analyte.....	8
Figure 3: Schematic of the pendant drop experiment showing the drop held inside the reservoir. Images are computer analyzed to determine the instantaneous surface tension.....	12
Figure 4: Volume versus surface tension as a drop of silicone oil is created in pure water. Above a volume of 50 μ L, the correct surface tension can be determined.	12
Figure 5. Rhodamine WT adsorption, first 5.5 hours.	14
Figure 6. Rhodamine WT adsorption, after 17 hours.	15
Figure 7. RWT desorption.	16
Figure 8. BSA Adsorption.	17
Figure 9. BSA Desorption. Arrows indicate when water additions were made.	18
Figure 10. CBM produced water adsorption.....	19
Figure 11. CBM produced water desorption.....	20
Figure 12. Prototype system schematic; 5 cSt PDMS oil injected into aqueous sample.....	21
Figure 13. Collapsed interface and jet for flow rates of 0.16 g/sec (a1 and a2), 0.19 g/sec (b1 and b2), 0.23 g/sec (c1 and c2), and 0.26 g/sec (d1 and d2).....	23
Figure 14. Calibration of the protein assay.....	24
Figure 15. Concentration of BSA in emulsion-processed water determined from absorption....	24
Figure 16. Test apparatus for sample injection into oil bath.....	27

TABLES

Table 1: Uncertainty analysis of surface tension calculation using pendant drop tensiometry.	13
Table 2. TDS measurements (sample conductivity, in microSiemens/cm) of interfacial filter processed and Millipore processed CBM processed water.	26

NOMENCLATURE

Bo	Bond number
BSA	Bovine Serum Albumin
CBMPW	Coal Bed Methane Produced Water
g	gravitational acceleration
PDMS	poly (dimethyl siloxane)
R	radius of pendant drop
ρ	density
γ	interfacial or surface tension

1. INTRODUCTION

Interfaces are known to have special properties because of their heterogeneous nature. One such property is that many varied materials are known to be attracted to and bind to them. We propose to harness this property to employ emulsions for interfacial extraction of materials from solution. In some ways, this is not a new idea. Activated carbon filters work in much the same way by exposing a large surface area which can adsorb the intended target material. However, we propose to use emulsions as “filters” where the interface between the two immiscible phases acts as the active surface area for adsorption. Emulsions have an obvious advantage over solid filters in that they can be easily regenerated by separating the two distinct phases through coalescence of the emulsion droplets. Because of this property, the amount of material waste generated can be significantly less when employing emulsion-based filtering.

We have investigated a novel emulsion interfacial filter that is applicable for a wide range of materials from small molecules and nano-particles to cells and bacteria, but which is expected to be particularly effective for proteins, viruses and similarly sized materials. The emulsion filter takes advantage of several characteristics of emulsions to efficiently trap and concentrate materials. First, a wide range of materials are attracted to interfaces between two materials, such as the surface of a droplet in an emulsion including proteins [1], cells including algae and bacteria [2,3], viruses [4], medically relevant materials such as cholesterol and caffeine [5,6], phenols [7], polymers including surfactants and lipo-polymers [8,9,10], hydrocarbons [11]. For many devices, this adsorption is a hindrance that leads to bio-fouling of surfaces and membranes as biological materials collect on the walls of the device. What is a hindrance in other circumstances will be utilized in our interfacial filter to trap and concentrate those same materials. Because affinity for adsorption to interfaces is ubiquitous, the emulsion filter can be applied to a wide range of biological and chemical materials of interest in homeland security and water surety applications [12].

The emulsion interfacial filter represents a significant break from traditional methods of concentrating samples and has the capability to be effective for a wide range of target analytes. At the same time it is complementary to the sample concentration methods currently under development at Sandia. Using emulsions is also a fundamental break from the extraction methods that have appeared in the scientific literature, including dielectrophoresis [13], isoelectric focusing [14,15,16], solid phase extraction [17,18], flow field fractionation [19,20], chemical affinity methods [21] and nano-capillary filtration. [22] This is a novel approach to the complex problem of sample concentration or filtration which offers significant advantages over the current proposed ideas. It is also a very unusual application for multiphase flow technology. While micro-emulsions have been used as a shape template for the manufacture of nano-particles [23] and other applications, no one has explored the possibility of using these emulsions as an interfacial filter.

Figures 1 and 2 depict the basic emulsion extraction concept with a two part concentration process. A small quantity of oil is mixed into the dilute sample, forming a dispersion of fine droplets. As the target molecules or particles diffuse into contact with the droplets, they are trapped by the attractive forces at the interface. Once the target material has adsorbed to the

interfaces in the emulsion of small droplets, the second stage of the process is concentration of the target by coalescence. By using controlled coalescence of the droplets, the interfacial area can be substantially decreased, resulting in an increase in surface concentration of the target of several hundredfold.

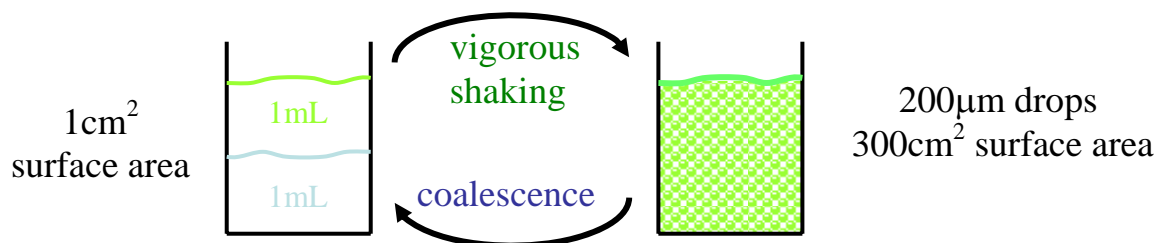


Figure 1: Using coalescence to collapse the emulsion interfaces and concentrate the target analyte.

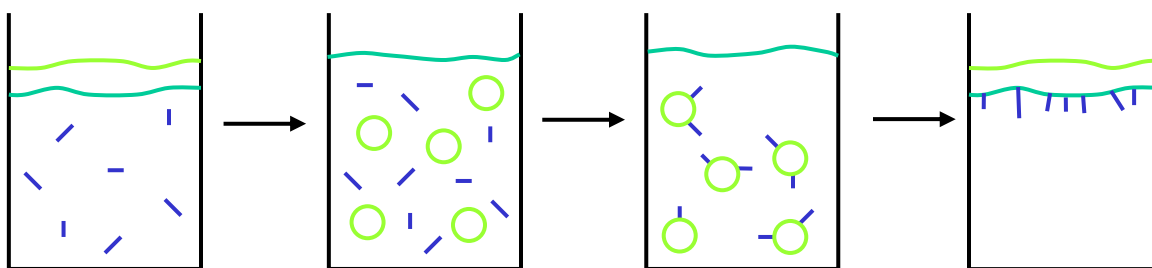


Figure 2: Formation of emulsion, trapping of the target material at the emulsion interfaces, and coalescence of the oil phase and concentration of the analyte.

We have investigated the promising capability of the emulsion interfacial filter as a novel method to extract and concentrate materials out of solution. The adsorption and trapping of materials at emulsion interfaces is demonstrated in Section 3 to verify the feasibility of interfacial extraction as a filtering technique. We then built a prototype interfacial filter that incorporates emulsification and coalescence processes which is described in Section 4. For these tests we used two types of systems: an aqueous solution of bovine serum albumin in buffer and coal bed methane produced water. We discuss lessons learned from our prototype system in Section 5.

2. MATERIAL TRAPPING AT EMULSION INTERFACES

We initiated our studies by developing methods to measure and quantify the trapping of materials at interfaces. There are two potential approaches; 1) measure the amount of material adsorbed at the interface and 2) measure the amount of material removed from solution. We have explored both possibilities with a variety of techniques. The majority of our experiments used measurement of interfacial tension as an indirect measure of the adsorption of materials at the interface, but we also explored Brewster Angle Microscopy as an option to directly measure surface adsorption. We have also directly measured the removal of material from solution using several techniques for different systems including the use of a spectrophotometer for fluorescent contaminants such as Rhodamine WT dye, performing protein assays to measure the concentration of a protein contaminant such as Bovine Serum Albumin, and total dissolved solids (TDS) testing to measure the concentration of dissolved ionic solids.

As an initial emulsion system we decided to use water and silicone oil. This system is immiscible and the silicone oil is inert, has a low viscosity and is non-toxic. For the aqueous phase, we used high purity water (NERL, Fisher), which is free from organic contamination and de-ionized to 18.2 megaohms. The silicone oil or poly(dimethyl siloxane) (PDMS) was purchased from United Chemical Technologies (Bristol, PA) and was used as received. The low viscosity (5 cSt) of the oil phase simplified emulsification. The interfacial tension between the two phases with no additives was measured to be 43 mN/m.

Our initial experiments were performed using several model systems which were representative of the range of materials that may need to be collected or removed from solution. We also tried to choose materials which would simplify quantitative detection. Our most complete experiments were performed on bovine serum albumin (BSA, Aldrich). This is a negatively charged blood plasma protein from cows that is used to regulate osmotic pressure.[24] It is commonly available at high purity and protein assays are available for accurate concentration measurement at low concentrations.

We have also applied our emulsion interfacial extraction idea to coal bed methane produced water (CBMPW). This water is a byproduct of methane extraction from shallow wells into coal formations. Disposal of the water, which may contain impurities such as salt and hydrocarbons, presents an environmental problem as does the resulting lowering of the water table. For a chemical analysis of the CBMPW, see Appendix A. Seven percent of the natural gas (methane) currently produced in the United States comes from CBM extraction.[25] Sandia is actively involved in research into alternative uses for the produced water created in the San Juan basin of north-western New Mexico.[26] The coal bed methane produced water used in our experiments was obtained through M. Hightower (06212) from the San Juan Basin of New Mexico.

The main experimental method which was applied to measure the adsorption of materials to the interface was measurement of the interfacial tension between the two immiscible phases using pendant drop tensiometry.[27] For this technique, a drop of one material is created inside the second liquid and imaged using a video camera. The shape of the drop is then fit to theoretical models to determine the interfacial tension using a custom-built LabVIEW program. Using this technique, we are able to track the dynamics of adsorption and desorption as well.

We have also explored using Brewster angle microscopy to directly measure surface adsorption. This technique involves illuminating the interface with a *p*-polarized laser from the side with the lower refractive index at Brewster's angle so that there is no reflection.[27] Once a material adsorbs on the interface, a portion of the incident laser light will reflect off the thin film formed at the interface. The intensity of the reflected beam is proportional to the thickness of the interfacial film. This technique has been applied quite successfully to measure the formation of films at the air-water interface [28] where the large density difference between the air and liquid keeps the interface very flat during the adsorption process. We believed that this technique would allow real-time monitoring of surface adsorption in our prototype system. However, in our emulsions, the difference in density between the two phases was much lower ($\Delta\rho\approx 0.1\text{g/mL}^3$), so the influence of gravity was relatively weaker. The interface between the two phases was highly curved and the decrease in surface tension caused by adsorption of materials at the interface resulted in significant variations in the interface shape. Thus, quantitative measurement of the reflected intensity was not feasible.

Three methods were used to directly measure decreases in concentration. When testing the surface adsorption of bovine serum albumin (BSA), we employed a BSA protein assay. In this procedure, a dye concentrate is added to a sample. Protein within the sample binds to the dye. The new dye:protein conjugate absorbs at 595 nm using an HP 8452a UV-vis spectrophotometer. The absorbance intensity is linear with protein concentration and can be measured with a UV-vis spectrophotometer. Second, measurement of Rhodamine WT dye concentration was determined by measuring the fluorescent intensity of the samples as compared to a calibration curve. For the tests involving coal bed methane produced water, the total dissolved solids present in each sample by measuring the conductivity through the water phase using a conductivity probe (TDS Testr 3, APT instruments). Results are presented in units of conductivity ($\mu\text{S/cm}$) because the complex chemical makeup of the CBMPW prevents direct conversion to traditional units of mg/L .

3. PENDANT DROP ANALYSIS

To measure the rates at which materials absorb and desorb from an oil-water interface, the dynamic interfacial tension was monitored using a pendant drop technique. Pendant drop is a well known technique for measuring surface tensions of liquids by creating a drop of the liquid suspended in air.[27] In this configuration, the adsorption of surface active materials in the liquid phase can be studied, but not the desorption kinetics. Recently, Svitova et al. modified the traditional pendant drop approach by generating a pendant air drop in a fluid reservoir. This way they were able to study both the adsorption and desorption dynamics at the interface by varying the concentration in the liquid reservoir.[29] Our interest is in studying the dynamics of liquid-liquid emulsions and there are special challenges with this system relative to air-liquid systems, such as the small density difference between the phases. Recently, Freer et al. used a pendant drop system to measure the adsorption of proteins to a hexadecane-water interface.[30] Our work for the first time studies the dynamics of adsorption and desorption of materials at a liquid-liquid interface. A diagram of the pendant drop experiment is shown in Figure 3. A glass reservoir holds the matrix liquid of interest. To measure the dynamic adsorption and desorption of materials, we can flow additional liquids into the reservoir using a peristaltic pump and/or drain liquid from the reservoir. Adsorption/desorption studies can be used to determine if materials are permanently bound to the interface or in dynamic equilibrium with the surrounding fluid.

A borosilicate capillary (Drummond Scientific, Broomall, PA; 25 μ L, 1.55mm OD) is inserted through a septum mounted in the bottom of the reservoir. The capillary is connected to a syringe pump (Harvard Apparatus PHD 22/2000 Remote Syringe Pump, Holliston, MA) which can be used to meter out small quantities of a second liquid (in this case silicone oil) to form a pendant drop. The shape of this drop is captured using a Cool Snap ES camera (Princeton Instruments, Trenton, NJ). The image is back-illuminated using a fiber optic light passed through several thicknesses of laboratory tissue, acting as a diffuser. The images were analyzed using custom software written in LabVIEW (National Instruments, Austin, TX).

To determine the surface tension, images of the plain capillary and the pendant drop are converted into a black and white image using a specified threshold. The initial blank image is used to determine the location of the end of the capillary. Then from the drop image, discrete points along the outline of the drop are identified. The drop shape is then fit to Laplace's equation to determine the surface tension. This method is very robust as long as the effects of gravity are sufficient to deform the drop shape (i.e. the Bond number defined as $Bo = \Delta\rho g R^2 / \gamma$ is sufficiently large, $Bo > 0.1$, that the drop isn't spherical). While this isn't typically of concern for measurements of the surface tension between liquid and air, the density difference for these two liquids is much smaller ($\Delta\rho=0.082$ g/cm³ versus ≈ 1 g/cm³). Figure 4 shows a plot of the calculated surface tension as a function of the volume for a drop of silicone oil being created in NERL water. Initially a drop was created and held to confirm that the surface tension was stable and then the drop was expanded to a final volume of 130 μ L. For very small drops the calculated surface tension is underestimated, but above 50 μ L ($Bo=0.11$), the surface tension is independent of volume. Over the final 40 images in the series, the average measured surface tension was 42.5 mN/m, with a standard deviation of 0.3 mN/m. For emulsion systems with smaller interfacial

tension or larger density difference, smaller drops are sufficient for accurate calculations of the interfacial tension. For the experiments discussed here, we used $50\mu\text{L}$ as the lower limit for drop size.

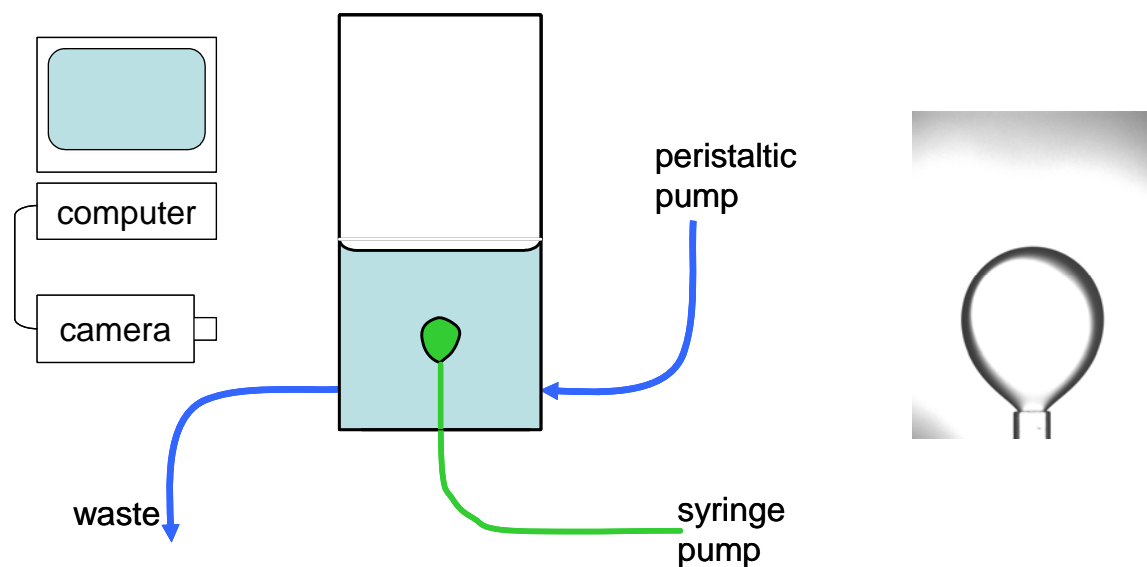


Figure 3: Schematic of the pendant drop experiment showing the drop held inside the reservoir. Images are computer analyzed to determine the instantaneous surface tension.

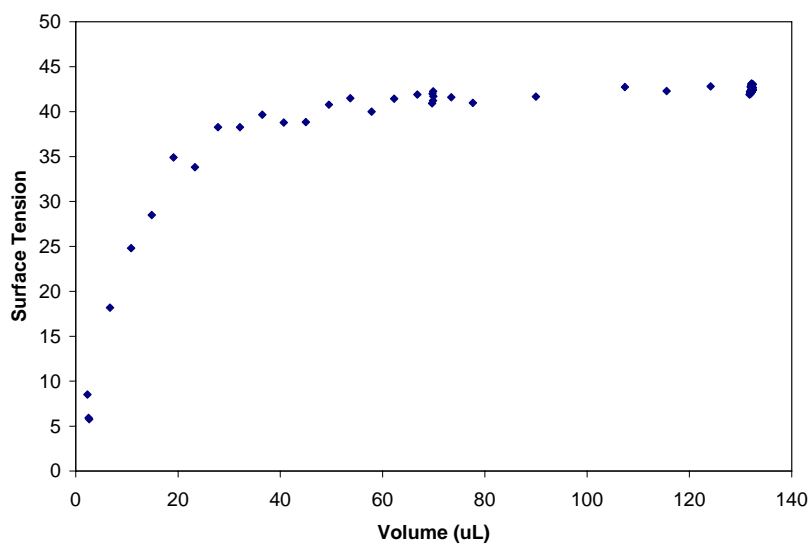


Figure 4: Volume versus surface tension as a drop of silicone oil is created in pure water. Above a volume of $50\mu\text{L}$, the correct surface tension can be determined.

We have also analyzed the effect of uncertainty in various input parameters for the surface tension calculation. Results for the three parameters, gravitational acceleration, density difference and image scaling factor, are summarized in Table 1. Gravitational acceleration has been adjusted for the relative altitude of Albuquerque, New Mexico and is known to high accuracy. The density of the test liquids were measured using a Mettler Toledo DE50 densitometer to within 0.001 g/cm^3 . However, since the difference in density between the two liquids is the required parameter, the uncertainty is increased to 0.002 g/cm^3 (or 2% uncertainty) and is a significant source of uncertainty in our calculations. The final parameter tested in the scaling factor used to convert image pixels to real world dimensions. For each test, the width of the capillary is used to calculate the scaling factor and can be determined to within 1 pixel, which is a 1.25% uncertainty. Since in this case the dependence on the parameter isn't linear, the scaling factor is also a significant source of uncertainty. So though we can calculate the surface tension with a repeatability of 1 mN/m , the uncertainty is closer to twice that value.

Table 1: Uncertainty analysis of surface tension calculation using pendant drop tensiometry.

Input parameter	Control Parameter	Deviation tested	Resulting deviation in surface tension	Expected uncertainty in parameter	Resulting uncertainty in surface tension
gravitational acceleration	979.2 cm/s^2	49 (5%)	5%	<1%	<1%
density difference	0.082 g/cm^3	0.004 (5%)	5%	2%	2%
scale calibration	574.2 pixel/cm	14.5 (2.5%)	5%	1.25%	2.5%

By analyzing the dynamic surface tension, we can probe the adsorption of materials to the interface. Many materials lower the surface tension when they adsorb; the most common example is surfactants.[27] By monitoring the surface tension versus time after a new oil drop is introduced to the aqueous phase, we can determine if any surface active materials are adsorbing to the interface. Once the surface tension has reached steady state, we can then add NERL water to the reservoir to dilute the aqueous phase and monitor the surface tension. If the surface tension remains steady, the material on the interface has irreversibly adsorbed. An irreversibly adsorbed material is an ideal target for interfacial extraction, because irreversibly adsorbed material will stay on the emulsion interfaces even as we collapse the interfaces through coalescence, simplifying extraction. If the surface tension increases when the aqueous phase is diluted, then the adsorbed material is reversibly adsorbed and the concentration on the interface is in dynamic equilibrium with the surrounding aqueous concentration. This means that the interfacial extraction process has to be fast relative to the desorption kinetics to be effective in removing that analyte.

Pendant drop testing results

As a reference point, the surface tension of air, 5 cSt silicone oil and 1000 cSt silicone oil in pure, nanofiltered (NERL) water were confirmed to be 72, 43, and 110 mN/m respectively. The air measurement and the 5 cSt silicone oil measurement were repeated at least 3 times with results within 1 mN/m of each other. In house deionized water, the surface tension dropped considerably in the first ten minutes and continued dropping to half of its original value after 48 hours, indicating that contaminants in the house deionized water were affecting the data. With nanofiltered NERL water, no reduction in the surface tension with 5cSt silicone oil was noted.

Adsorption of Rhodamine WT (RWT) dye

In the data graphed in Figure 5, 9 mL of 8.1×10^{-9} M RWT dye in house deionized water was added to 800 mL of NERL water. The initial data shows the growth of the 5cSt silicone oil droplet to a final volume of 140 μL , and then the drop was observed for an additional 20 minutes with no apparent decrease in surface tension. The initial trend upwards occurred as the drop was being created, but once the drop volume was steady, the surface tension was approximately constant at 43 mN/m, equivalent to the pure water measurement. An additional 13.3 mL 1.62×10^{-8} M RWT dye was added after 17 hours (for a final concentration of 3.5×10^{-10} M RWT dye) in the hopes of seeing a change in the measured interfacial tension. The water was slightly pink after this second addition. However, only a slight increase in the interfacial tension was apparent which was within the uncertainty of the measurement as shown in Figure 6.

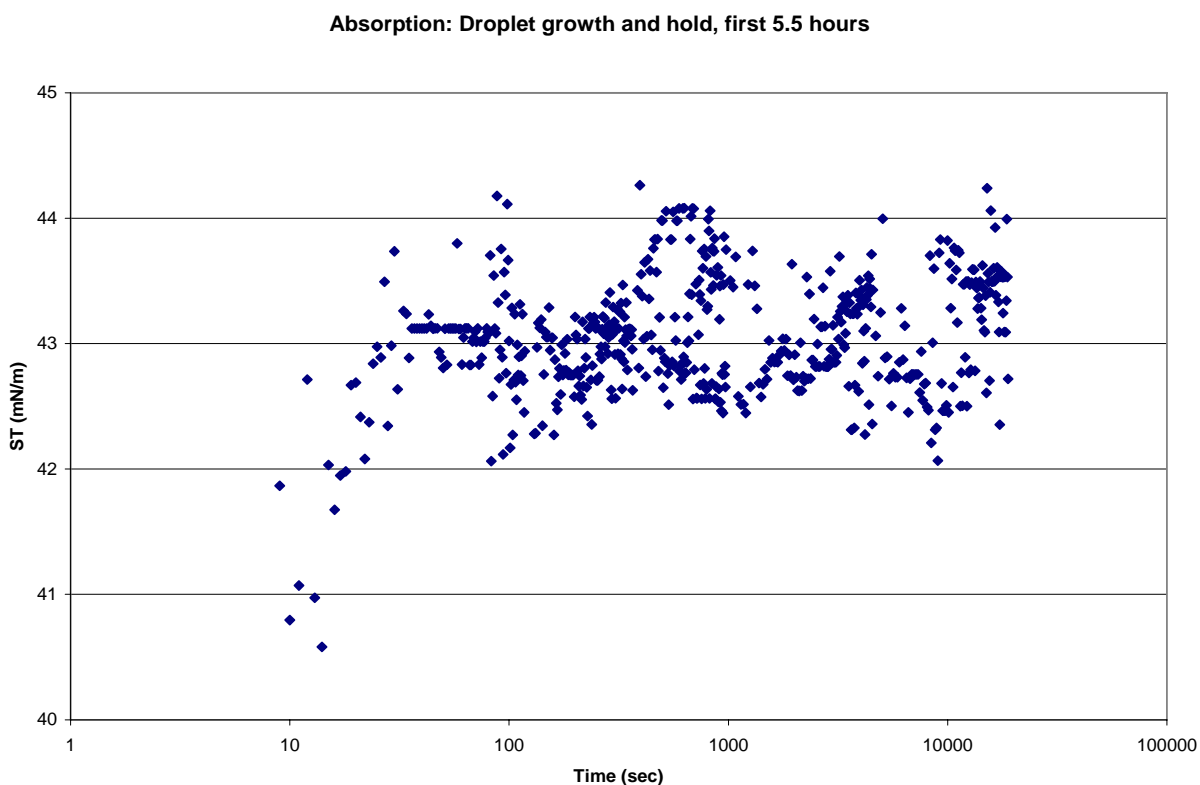


Figure 5. Rhodamine WT adsorption, first 5.5 hours.

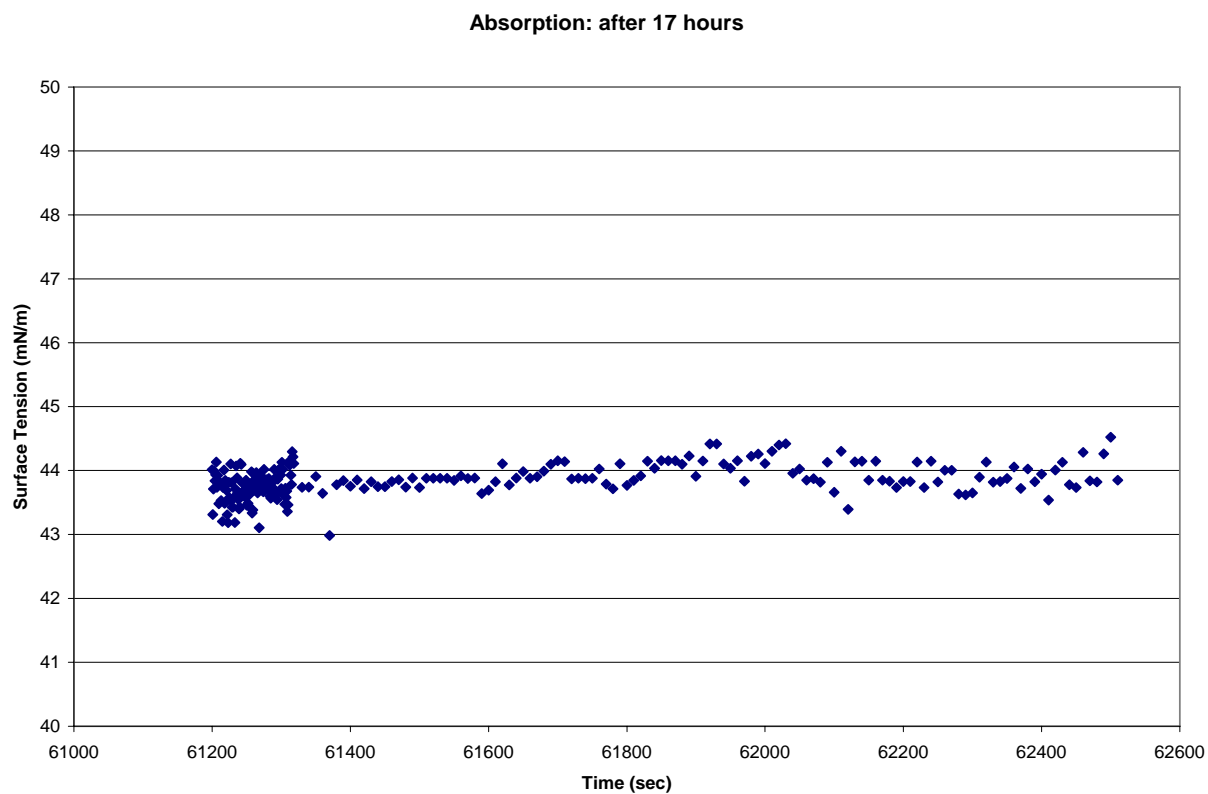


Figure 6. Rhodamine WT adsorption, after 17 hours.

Desorption of RWT

A 130 μL droplet of the 5 cSt oil was created on the tip of the capillary and held for four hours to ensure that equilibrium had been reached with the 3.507×10^{-10} M concentration RWT solution. At the beginning of data collection shown in Figure 7, 1.8 liters of NERL water was flowed into the vessel over 4 hours (14400 sec) using a peristaltic pump. Over the course of the experiment, some solution was also drained from the outlet port. While liquid is being pumped into the reservoir, the drop experiences some vibration and the error in the calculated surface tension increases. The measured surface tension is approximately constant, varying within $\pm 1\text{mN/m}$ which is within the uncertainty discussed above. Our conclusion is that this fluorescent dye either does not adsorb at the interface, or does not affect the surface tension if it does adsorb.

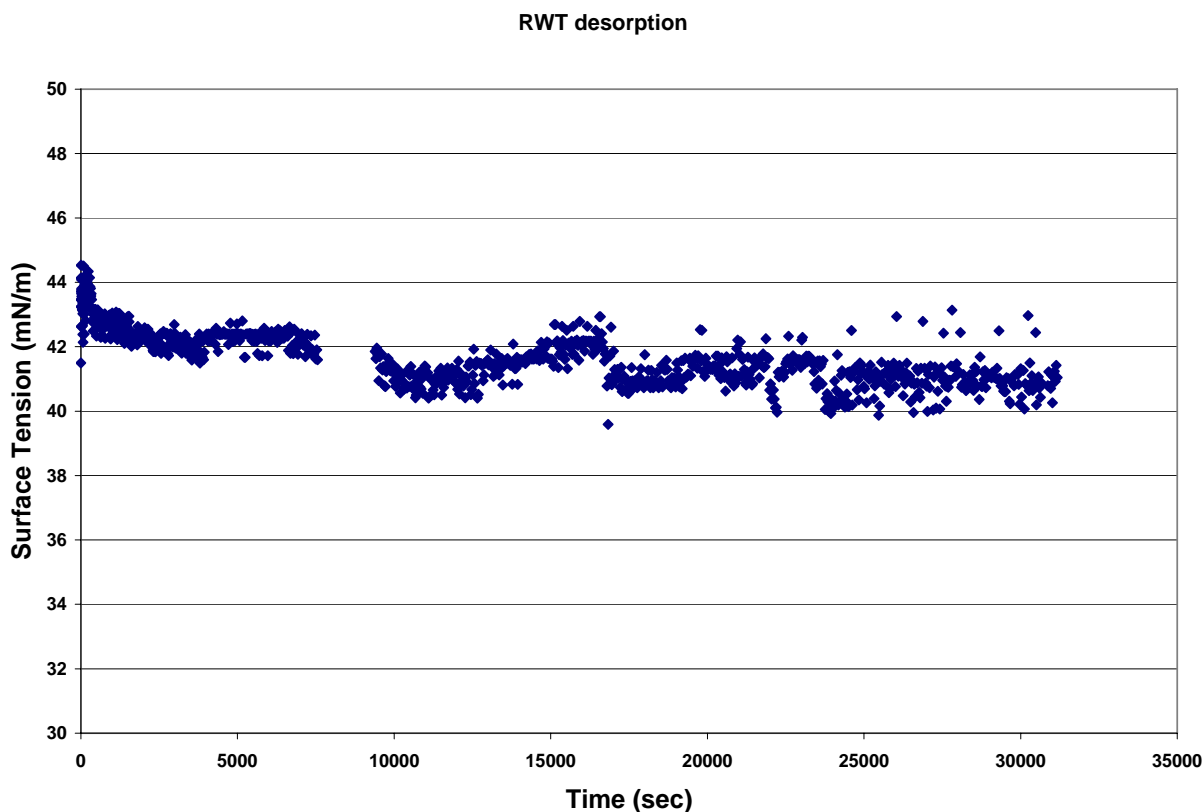


Figure 7. RWT desorption.

Absorption of Bovine Serum Albumin (BSA)

Solutions bovine serum albumin were prepared by combining 0.1 g BSA (Aldrich) with 1 Liter of 0.0001 M NaCl in NERL water. The vessel was stirred with a stir bar to dissolve the solid BSA. Prior to adding the BSA, the surface tension of an oil droplet in the salt water was confirmed to be constant (c.f. Figure 8) though slightly below the pure NERL water surface tension. Using 5 cSt PDMS oil, a droplet with a volume of 60 μL was pushed out of the capillary and held while taking images. The measured interfacial tension of the droplet rises as the droplet is being created, then it begins dropping once the final volume is obtained. The surface tension drops 20 mNm in less than 3 hours, with a noticeable drop occurring after only 1.5 minutes. For this case the surface tension does not appear to reach steady state, which is consistent with other similar measurement in the literature using an air–water interface.[32]

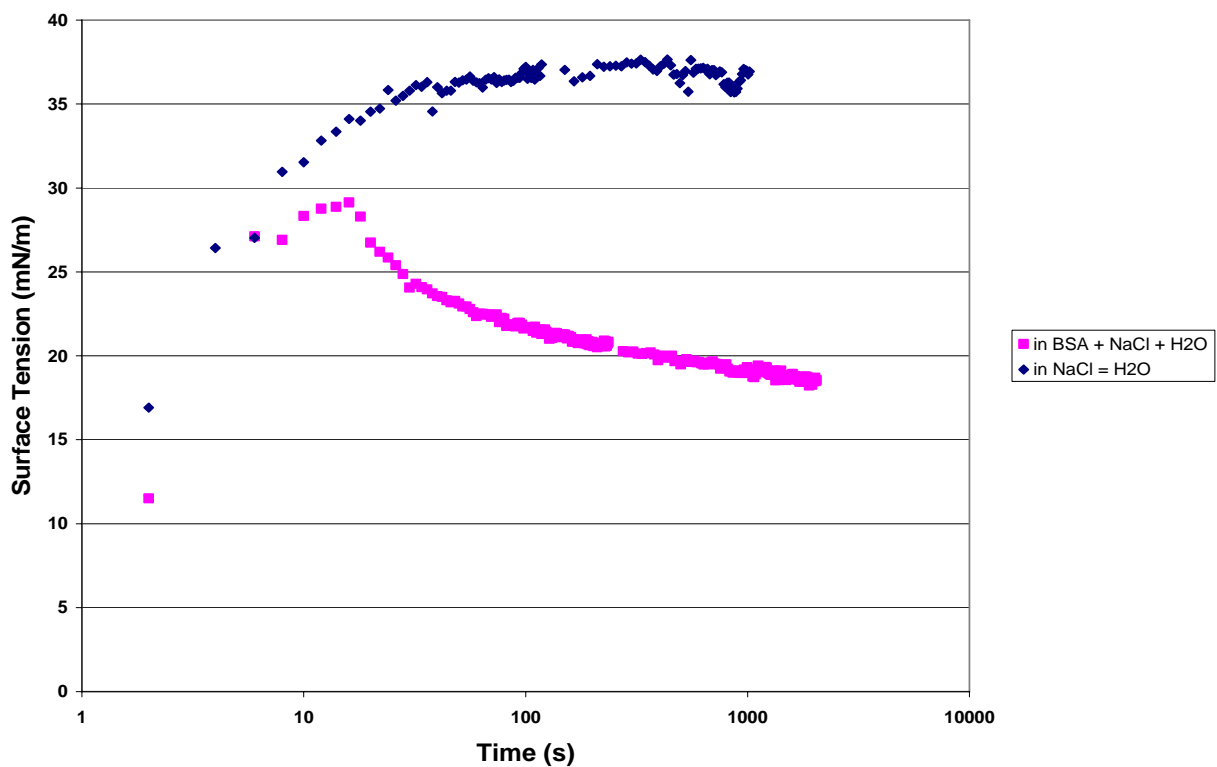


Figure 8. BSA Adsorption.

Desorption of BSA

To determine how strongly bound the BSA was to the interface, we performed a desorption experiment. An oil drop was created and allowed to equilibrate with the BSA solution for an hour (3600 sec). Then 0.0001 M NaCl in NERL water was flowed into the vessel using a peristaltic pump. Over the course of the data below, 2 Liters of salt solution was added to our original volume of 1.023 L BSA solution in 600mL increments. The starting points for each addition of salt solution are marked on Figure 9. No desorption is visible, indicating that the BSA could be easily trapped and removed using our emulsion interfacial filter.

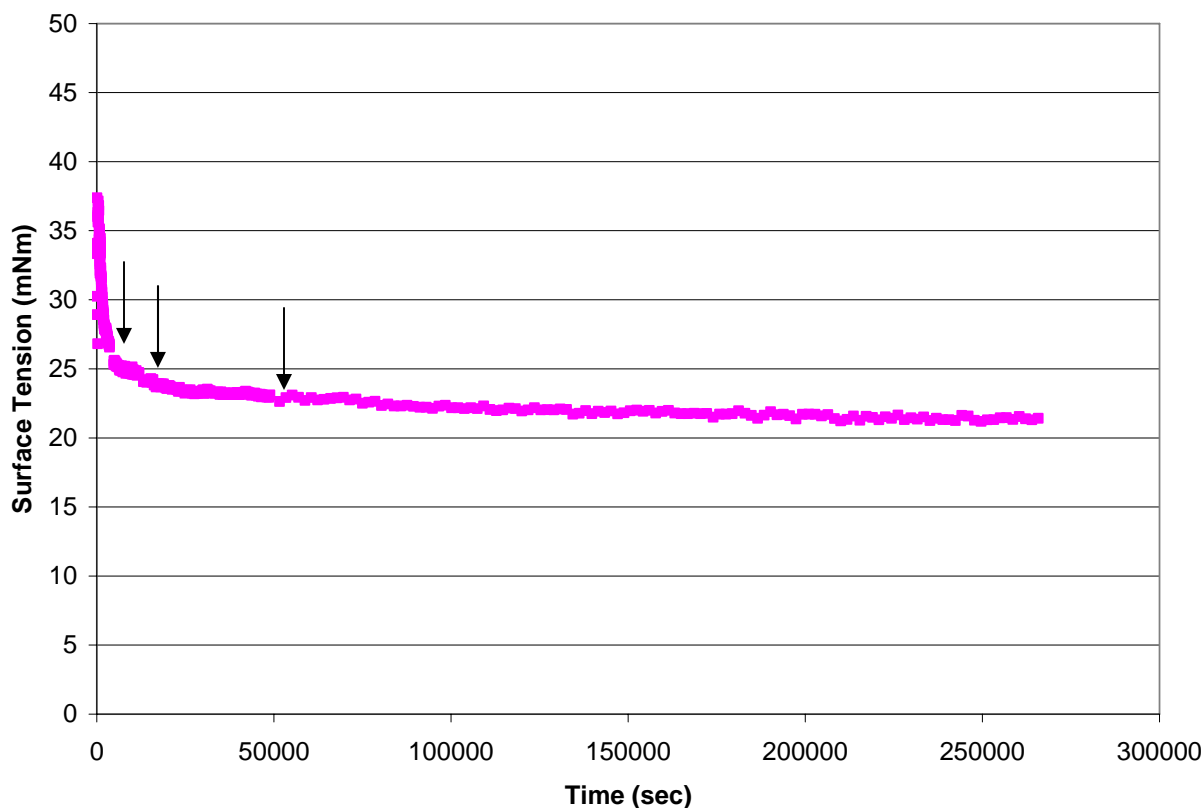


Figure 9. BSA Desorption. Arrows indicate when water additions were made.

Absorption and desorption of CBM water

We also performed pendant drop analysis on the coal bed methane produced water. The data in Figure 10 shows the surface tension of a 44 μL droplet that was exposed to coal bed methane produced water (CBM water). A much smaller volume droplet had to be used for this experiment, since the drops experience such a large decrease in surface tension that larger droplets would disconnect from the glass capillary. After 4.5 hours, the surface tension of the droplet had dropped to 18 mN/m, and had not yet stabilized. Though the composition analysis (Appendix A) does not indicate what materials may be adsorbing at the interface, there is clearly a significant concentration of surface active material. There was significant variation in the measured interfacial tension dynamics with the coal bed methane water, due primarily to the sample variability. For example, the data shown in Figures 10 and 11 were taken with different CBMPW batches, and have different equilibrium values of the interfacial tension. Over a period of over a day, the interfacial tension drops to ~ 19 mN/m. To determine how strongly adsorbed the compounds are to the interface, we diluted the CBMPW by half adding NERL water; see Figure 11. While the water is being added over the course of 30 minutes, there is a jump of 3 mN/m in the interfacial tension, but then the interfacial tension slowly decreases back to within 1 mN/m of the previous value. Since the variations in the interfacial tension are small compared to the decrease from the pure water interfacial tension of ~ 35 mN/m, we conclude that most of the material is strongly adsorbed to the interface and could be removed by an emulsion interfacial filter.

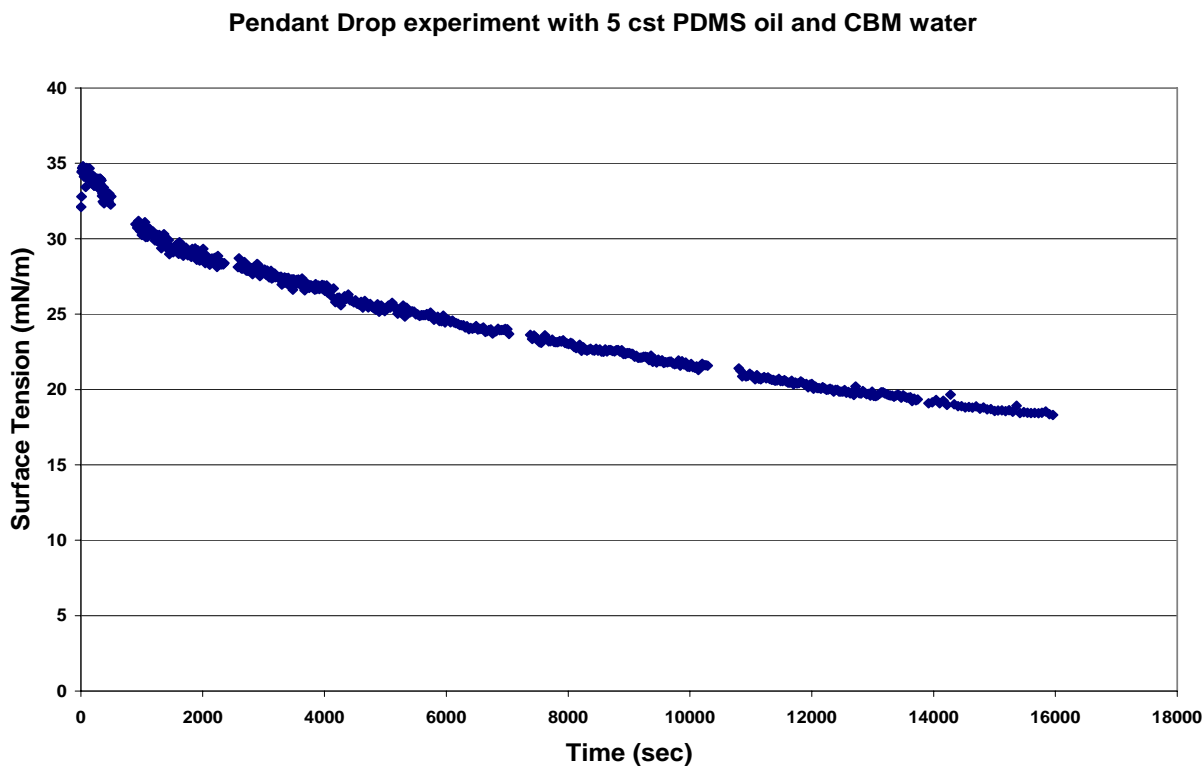


Figure 10. CBM produced water adsorption.

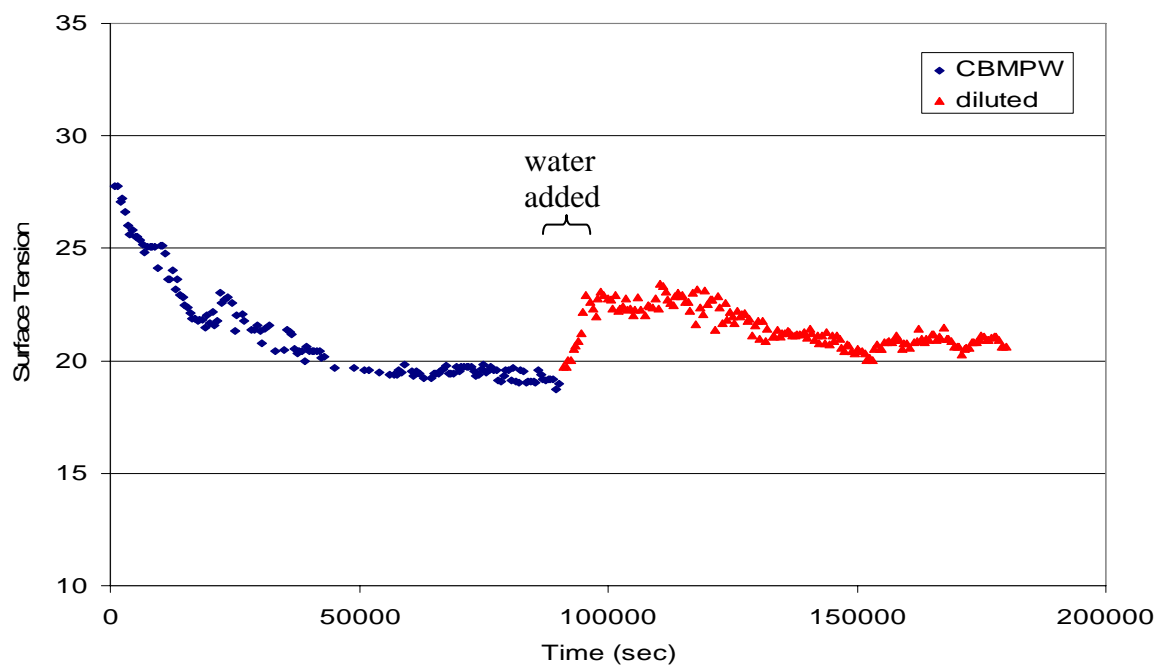


Figure 11. CBM produced water desorption.

4. PROTOTYPE SYSTEM ANALYSIS

In order to demonstrate the capability of emulsion technology to be an effective system filter, we performed a series of tests. The test apparatus, shown in Figure 12, was a two-inch diameter cylindrical glass vessel with an entrance port located approximately $\frac{1}{2}$ inch above the vessel's floor. The entrance port was fitted with a septum, through which both an injection needle and a sample extraction needle could pass. For all of the tests performed here, a flat-tipped stainless steel dispensing needle (EFD Inc, East Providence, RI) was used, with a 0.33 mm inner diameter and 0.64 mm outer diameter. By varying the needle size, the oil drop size of the emulsion can be varied, though we found it more convenient to adjust the drop size using the oil injection speed.

The vessel was filled with 200 ml of aqueous sample, and approximately 50 ml at a time of 5 cSt PDMS oil was injected into the sample through the injection needle via a peristaltic pump. At very low injection velocities, very large drops were formed, similar to the pendant drop experiment, and very little mixing was achieved between the phases. For these measurements, we employed a range of higher oil injection rates, from 150-300 mg/sec. For this entire range, a jet of oil droplets is injected into the vessel, which penetrates the entire width of the vessel. Images of both the droplet jet formed while the oil is injected and the interface after all of the oil droplets have coalesced are given in Figure 13 for four of the cases tested. After the emulsion at the interface between the oil and water phases had collapsed, the interface between the two phases was imaged as shown in the left side of Figure 13. Note that a film is discernable at the interface for all of the flow rates tested.

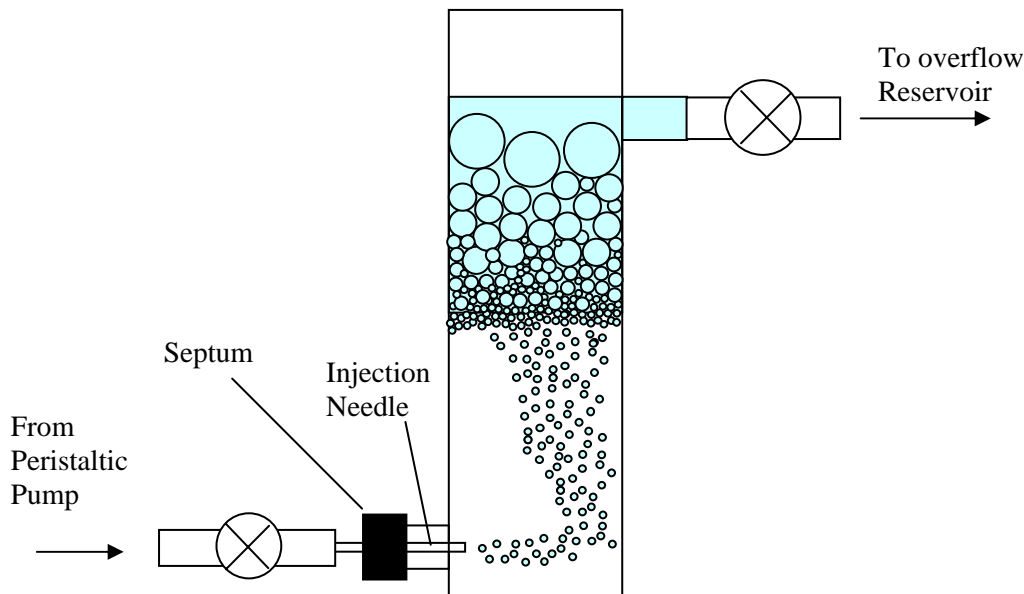


Figure 12. Prototype system schematic; 5 cSt PDMS oil injected into aqueous sample.

After the sample-oil emulsion had collapsed, a test sample was extracted from the sample volume for testing. These results will be presented on the following pages. Two sample fluids were tested in this manner; a 200 ppm BSA in NERL water solution with a NaCl buffer, and coal-bed methane produced water from the San Juan basin of north-western New Mexico.

Oil Jet Characterization

At the slower oil injection rates that we used in our tests (0.16 and 0.19 g/sec), a jet of uniform oil droplets is injected into the sample solution, which penetrates the entire cross-section of the test apparatus before drifting up to the top of the sample, where the droplets coalesce. For a flow rate of 0.16 g/sec, as shown in Figure 13 a2, the jet produces oil droplets 1.25 to 2 mm in diameter. For flow rates above 0.20 g/sec, the mechanisms which govern the droplet's formation become unstable, and the oil droplet size distribution becomes quite broad. For example, at a flow rate of 0.23 g/sec (Figure 13 c2), the oil droplet sizes range from 0.2 to 2 mm. In addition, enough momentum is transferred to the sample in the vessel that the bulk fluid begins to swirl. At the highest injection flow rates, the speed at which the smaller droplets are traveling is sufficient to allow them to swirl around the vessel many times before they float to the top of the sample. Therefore, we see that both the surface area available for interfacial extraction of materials and the volume of the sample readily mixed with the oil droplets increases with increased injection rates. When very small (less than 200 micron) droplets are formed, though, the time necessary for all droplets to reach the interface and then coalesce is increased considerably. Buoyancy forces drive the oil droplet towards the oil layer and the coalescence of droplets is highly dependent on the droplet's radius of curvature. When operating the system at flow rates in excess of 0.25 g/sec, the sample would still appear cloudy due to the presence of fine oil droplets for up to an hour after oil injection was stopped.

BSA Assay Summary

We wanted to test the ability of the oil-water emulsion to remove BSA from water. The experiment was initiated with a 200 ml solution of 200 ppm BSA in 1×10^{-4} M NaCl in NERL water. 5 cst PDMS oil was injected into the vessel at a rate of 0.25 g/sec. This speed setting resulted in very turbulent mixing in the glass vessel, roughly equivalent to that shown in Figure 13 d2. The stopcock at the top of the vessel was left open to allow excess oil to flow out into an overflow reservoir. Oil was injected into the test apparatus until a total amount of oil equal to 50 grams, 100 grams, 200 grams, 400 grams, and 505 grams was injected; at which point the experiment was paused. During each pause, the oil-water mixture was allowed to coalesce for at least 1 hour to allow the oil and water phases to separate completely. A water sample was then extracted from the water phase by plunging a pipette through the oil layer. While inserting the pipette through the oil layer, air was being ejected from the pipette to limit the amount of oil gathered in the sample.

A protein assay was used to measure the concentration of BSA in the water phase. Using sterile cuvettes, pipette tips, and vials, 50 μ L of sample (or standard) was mixed with 2.5 mL of the diluted protein assay concentrate. The cuvette was then vortexed and allowed to sit for at least 5 minutes, but not longer than an hour. The absorption at 595 nm is then measured for all samples that have been prepared, as the absorption in a sample will increase with time. A standard calibration curve was generated from 5 concentrations, with each concentration sampled 3 times. This procedure established both the calibration and the uncertainty associated with the technique. The calibration is shown in Figure 14. For the range in concentration over which the calibration was gathered, a linear fit was accurate to within a fitting value (R^2) of 0.998. The uncertainty in the sample intensity, based on spread of intensity values gathered at each concentration, appears to be +/- 5%.

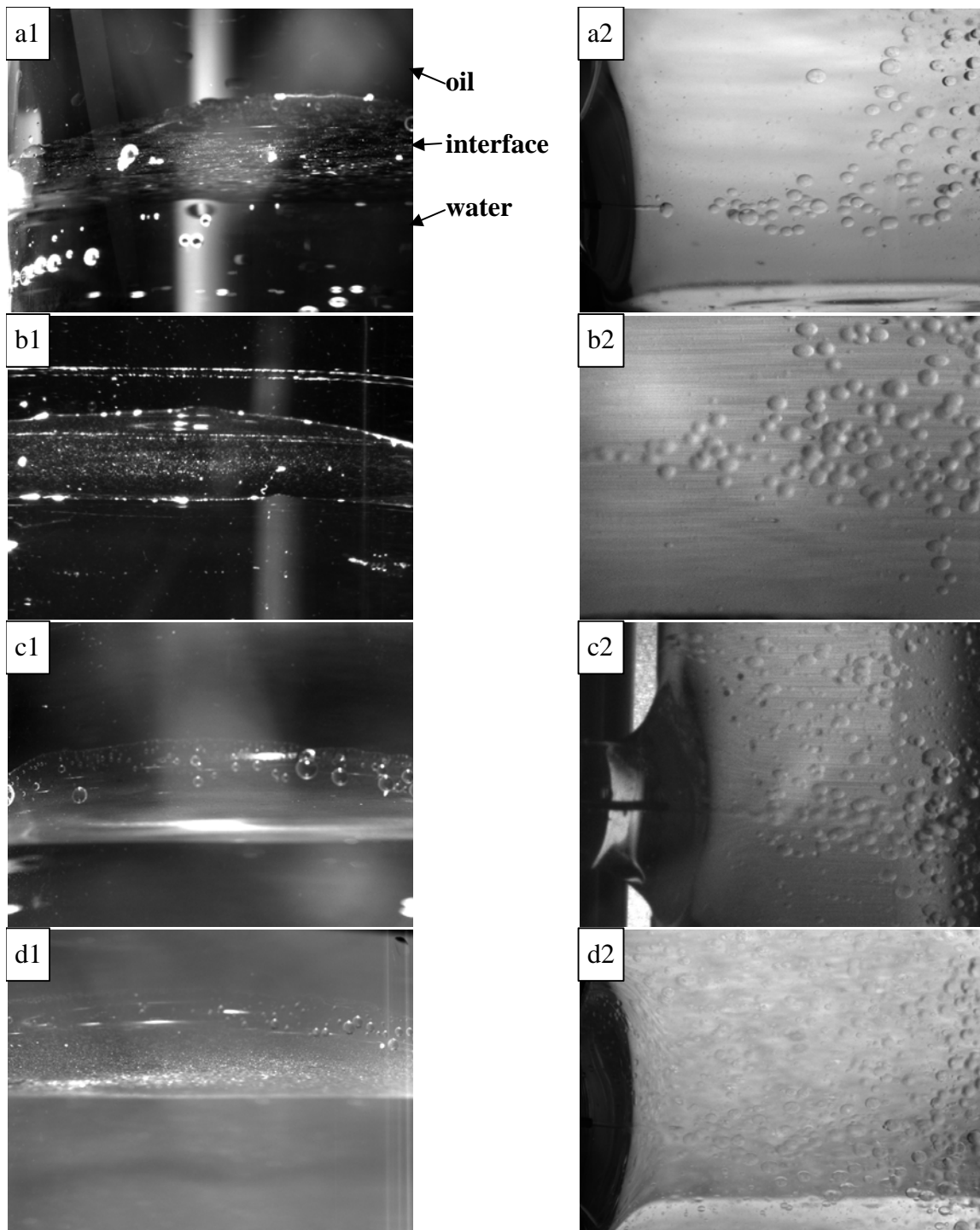


Figure 13. Collapsed interface and jet for flow rates of 0.16 g/sec (a1 and a2), 0.19 g/sec (b1 and b2), 0.23 g/sec (c1 and c2), and 0.26 g/sec (d1 and d2).

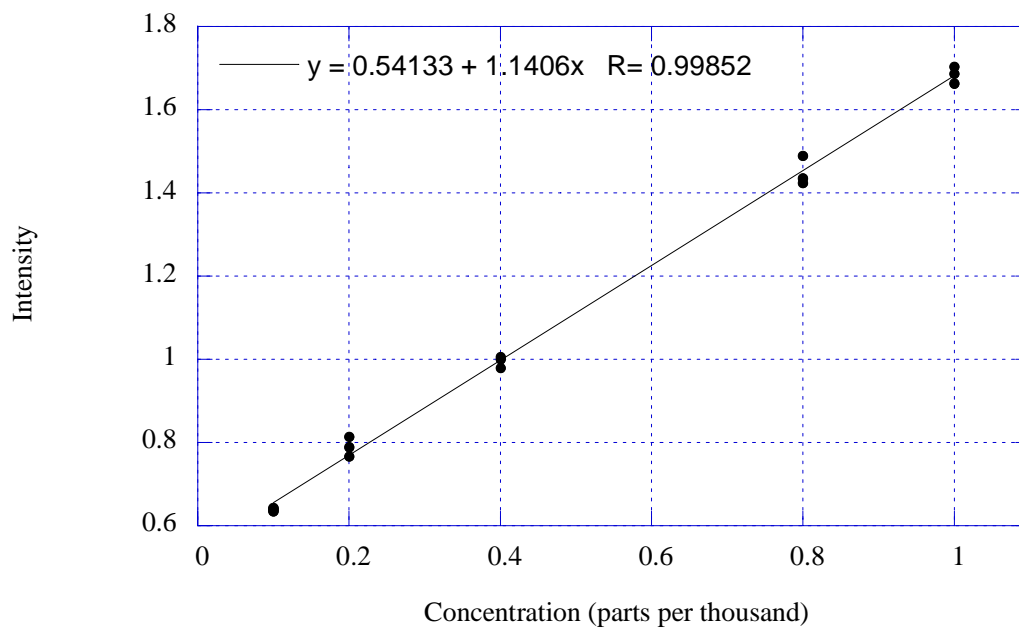


Figure 14. Calibration of the protein assay.

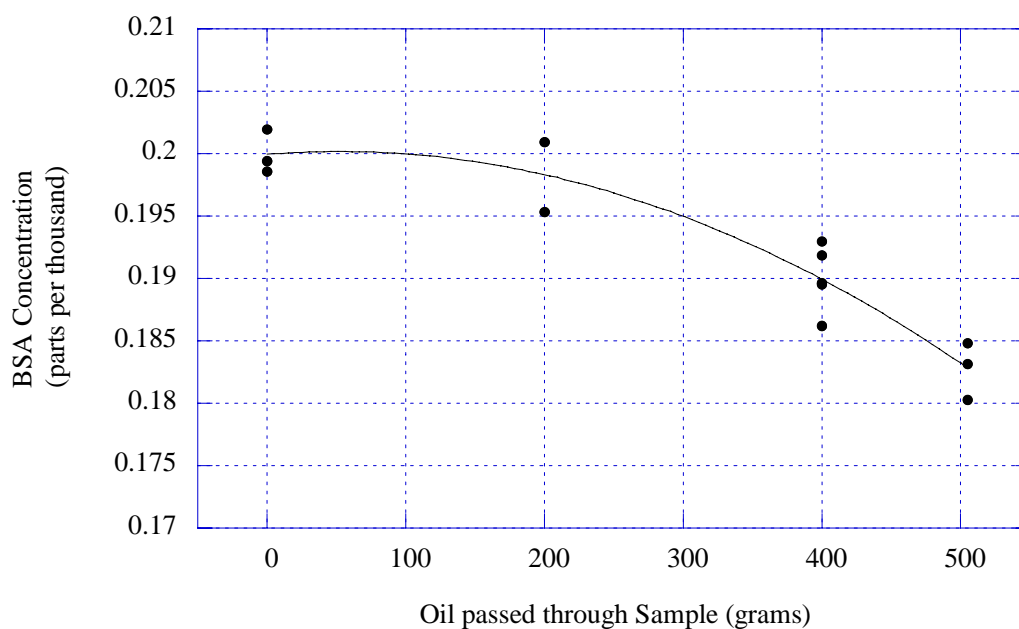


Figure 15. Concentration of BSA in emulsion-processed water determined from absorption.

The results of these tests are shown in Figure 15 for 200, 400, and 500 grams of PDMS oil passed through the test apparatus. There does appear to be a noticeable and systematic drop in

BSA concentration with increased oil passing through the system. The BSA concentration has dropped by approximately 8.5% after 500 ml of PDMS oil droplets have been passed through the system. The systematic drop in BSA concentration indicates that significantly more BSA can be extracted by increasing the interfacial area available for BSA absorption and/or the contact between the two phases. The interfacial area can be increased by either increasing the amount of oil passing through the system (i.e., running the jet longer), or decreasing the droplet size.

Emulsion-filtering of CBM produced water

With the CBMPW, it was difficult to directly determine what was being removed from the system. A chemical analysis performed on the water (Appendix A) details the main solutes such as sodium chloride salt, and indicates that there were no detectable dissolved hydrocarbons. However, the pendant drop indicates that there are clearly dissolved substances present in the water which adsorb to the oil water interface, reducing the measured interfacial tension. To quantify how much material we were removing from solution with our interfacial filter, we employed total dissolved solids testing. TDS is used to measure the “dirty”-ness of the produced water by measuring the conductivity which accounts for salts and other ionic compounds. Presumably, the decrease will be due to removal of larger charged species from solution. Therefore, we compared the performance (via TDS measurements) of the interfacial filter to filtration of the CBMPW using a 0.22 micron Durapore membrane filter. Since neither filter is expected to remove small molecules including sodium and chloride, comparison of relative performance seemed the best way to judge if the interfacial filter was effective. We used a Millipore Hazardous Waste Filtration System (Millipore Corporation, Billerica, MA Cat. No. YT30 142 HW) with two types of filters: a Durapore 0.22-micron membrane filter and a glass fiber filter without binder (AP40). Unfortunately, the glass fiber filters were difficult to work with because they were fragile and the o-ring seal would cut through the filter when mounted in the filtration system. The Durapore filters were more robust and had a very small pore size relative to the glass fiber filters, so these were used for our comparison testing.

Additionally we explored the related total suspended solids (TSS) testing as a method for quantifying the effectiveness of the interfacial filtration prototype, but after careful consideration, opted against pursuing TSS testing for quantitative measurements. The sample volumes of CBMPW that we were using (200 ml) and the amount of contaminants present that we are able to extract with either the interfacial filter or the Millipore filtration system had dictated that the weight of filtered material would be very small in relation to the weight of the Durapore filter, and therefore very difficult to measure accurately and consistently.

To assess the performance of the emulsion interfacial filtration prototype, TDS measurements were performed on CBMPW which had been processed through our prototype. For these experiments, 50 grams of 5 cSt PDMS oil was injected at a rate of 0.29 grams/sec into a 200-ml CBMPW sample. The TDS results of the interfacial extraction filtrate were compared to TDS reading of un-filtered CBMPW water and also CBMPW water which had been filtered using the Durapore membrane filter. The results of these tests are shown in Table 2. The interfacial filter performed favorably compared to the membrane filter, decreasing the TDS measurement by approximately 80% of the amount the Durapore filter decreased the TDS reading, decreasing the total dissolved solids by 10% from the un-filtered water. To determine if the two techniques were removing the same material from the CBMPW, we took the filtrate from the interfacial filter and passed it through a Durapore filter. When accounting for the uncertainty of the TDS

measurement (± 200), there was no significant change in the measured TDS between the interfacial filter + Durapore filtered and Durapore filtered only samples, indicating that the two methods were removing the same charged species from the CBMPW. Additionally, our interfacial filter technique has advantages in that unlike a solid filter, the oil phase is recovered while the contaminant remains trapped at the oil-water interface.

Table 2. TDS measurements (sample conductivity, in microSiemens/cm) of interfacial filter processed and Millipore processed CBM processed water.

	Un-filtered CBMPW	Interfacial Filter processed water	Durapore filter processed water	Interfacial Filter and Durapore filter processed water
Sample 1	15570	13920	13280	13640
Sample 2	15615	14000	13760	13840
Sample 3	15660	14080	13600	13840
Average	15615	14000	13547	13773

5. EMULSION SYSTEM DESIGN

From our process of operating the prototype emulsion interfacial filter, several lessons learned have become apparent which would enhance the efficiency of the device in real world applications. One notable enhancement would come from changing how the emulsion is created. Currently, we are dispersing the oil into the aqueous phase by using a small needle to generate drops of oil. Those drops are then mixed with the aqueous phase to enhance contact of the analyte with the interfaces. This was useful so that we could study the effects of more interfacial contact and mixing as the oil droplets were smaller or more oil droplets were passed through the aqueous liquid. However, in our system, we operated on a certain volume of water at a time.

For application to real world, operation would be much simplified by reversing the emulsion and creating water droplets in an oil matrix. The test apparatus would be identical to that shown in Figure 12, except that the aqueous sample would be injected into the oil phase through the top port, and allowed to settle and coalesce at the bottom of the reservoir, as shown in Figure 16. This configuration would have several advantages. First is that the water could be processed in a continuous manner (rather than the batch processing above). Second, because of the mixing characteristics, the liquid inside the droplets has better contact with the interfaces (shorter diffusion length), so having the aqueous phase inside the droplet would enhance transport of the analyte to the interface. Third, since the water phase has a lower viscosity, smaller droplets may be created when dispersing the aqueous phase. Finally, depending on the nature of the aqueous phase being considered, electrostatic repulsion forces can hinder coalescence of oil drops in an aqueous medium. This is advantageous in this instance because it will increase the time available for the target analyte to reach the interface and bind before the droplet coalesces.

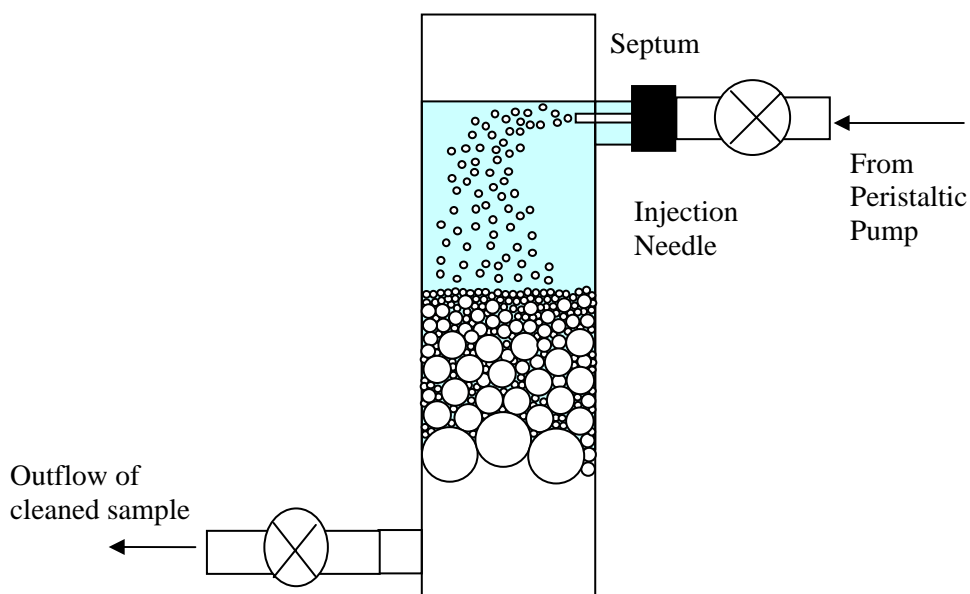


Figure 16. Test apparatus for sample injection into oil bath.

Increasing the height of the reservoir would also increase the mixing interaction between the two immiscible phases. That would allow the emulsion droplets more time as they rise (for oil droplets) or settle (for water droplets) through the other phase. That would increase the time available for diffusion of the target analyte to the emulsion interfaces.

Another change which should be considered is the choice of oil. Silicone oil was an obvious choice because it is environmentally benign, and is strongly immiscible with water. The grade of oil chosen for this work was the lowest available viscosity (5cSt). The low viscosity allowed us to generate a fine spray of oil droplets as shown in Figure 13. However, some concerns were raised that this low molecular weight of oil may be slightly volatile. The 20cSt grade of silicon oil has no vapor pressure and may be a better choice in the future. If the droplets are created from the water phase as discussed above, we can still create a fine spray of water drops even in a more viscous oil. Additionally, a higher viscosity oil phase will increase contact times between the oil and water phases by slowing the settling of water drops through the oil and slowing the coalescence of the water droplets. This will be beneficial in encouraging trapping of materials at the interface.

Our experience with the fluorescent RWT dye also suggests that not all chemicals can be attracted by all emulsions. In this case, either the dye did not affect the surface tension, or more likely the dye did not adsorb at the oil-water interface. The two other test cases which were studied, the protein solution and the coal bed methane produced water, both adsorbed strongly to the silicone oil–water emulsion interfaces. Obviously, if the material of interest does not adsorb to the interface, the emulsion interfacial filter will not be effective. However, the emulsion interfaces can be tailored to be more attractive to specific compounds. Specifically, by adding tailored surfactants which reside at the oil-water interfaces, you can change the chemical nature of the emulsion interface to attract and bind specific compounds.

6. CONCLUSION

Our project sought to test a novel idea to use oil-water interfaces in an emulsion to trap and remove contaminants from one of the phases. We have successfully demonstrated that emulsions do trap materials and we have built a prototype device to apply the emulsion interfacial filter concept. There are many fields where removing and/or collecting samples is important. We have applied our technique to clean up of coal bed methane produced water which is one example in the energy applications area. This technique could also be used as part of sample collection for sensors or as a part of waste water processing.

This technique has many similarities to traditional solid filter technologies such as carbon filter technologies. Both use heterogeneous interfaces to adsorb materials out of solution. However, the emulsion interfacial filter has a very clear advantage—these systems are easily cleaned. When the interfaces are full of contaminant, the emulsion can be collapsed into the two immiscible phases, concentrating the contaminant at the interface of the two phases and recovering clean liquids. This will generally happen spontaneously. Solid filters, after they are saturated with contaminant, are typically disposed of or have to be regenerated at high temperatures or with chemical treatments (creating in some cases hazardous waste). Since our emulsions have dynamic interfaces, they are easily regenerated, leaving behind all of the contaminated interfaces.

We successfully proved the ability of emulsion interfaces to effectively collect and trap materials from aqueous solution. We tested two aqueous systems. The first was a solution of 200ppm bovine serum albumin (BSA), a common negatively charged protein. The second was coal bed methane produced water (CBMPW) from the San Juan Basin. This complex waste brine mixture is a byproduct of methane production in north western New Mexico and Sandia is actively seeking methods to cheaply and efficiently clean it up so that it can be recycled.

Using a pendant drop technique to dynamically monitor the interfacial tension, we tracked the adsorption and desorption of materials at the oil-water interface. Once the interfacial tension had stabilized, the aqueous phase was diluted with NERL water while monitoring the interfacial tension. If the interfacial tension remained constant this indicated that the material was irreversibly adsorbed and could be effectively removed from solution with the emulsion. Both the BSA and CBMPW showed large changes in the interfacial tension as molecules from aqueous solution adsorbed onto the oil-water interface. For the CBMPW, water chemistry analysis leaves us unclear exactly what chemical compounds are extracted from the water. Upon dilution of the aqueous phase with pure water, the BSA remained adhered to the interface resulting in no change in the interfacial tension. For the CBMPW, there was a slight increase in the surface tension, but the interfacial tension remained significantly lower than for pure oil and water.

We also built a prototype system to test the emulsion interfacial filter concept. We created a small reservoir which could hold 200mL of aqueous phase. An emulsion was created by introducing the oil phase through a small stainless steel square tipped needle (0.33 mm ID). At low flow rates, the oil created large drops which did not provide much mixing with the aqueous

phase. At higher flow rates (250 mg/s), the oil creates a turbulent spray of droplets which causes vigorous mixing with the aqueous phase. For the BSA system, protein assay showed a progressive decrease in the residual BSA concentration with more mixing of the two phases.

With the CBMPW, it was difficult to directly determine what was being removed from the system. A chemical analysis performed on the water (Appendix A) details the main solutes such as sodium chloride salt, and indicates that there were no detectable dissolved hydrocarbons. However, the pendant drop indicates that there are clearly dissolved substances present in the water which adsorb to the oil water interface, reducing the measured interfacial tension. To quantify how much material we were removing from solution with our interfacial filter, we employed total dissolved solids testing. TDS is used to measure the “dirty”-ness of the produced water by measuring the conductivity which accounts for salts and other ionic compounds. Therefore, we compared the performance (via TDS measurements) of the interfacial filter to filtration of the CBMPW using a 0.22 micron Durapore membrane filter. Since neither filter is expected to remove small molecules including sodium and chloride, comparison of relative performance seemed the best way to judge if the interfacial filter was effective. The interfacial filter performed favorably compared to the membrane filter with both techniques showing ~10% decrease in the total dissolved solids.

During operation of our initial prototype, several lessons learned have been discovered which would improve application and scale-up of this technique. Most critically, we recommend reversing the emulsion to create water drops in an oil matrix. This change would significantly increase contact between the aqueous phase and the emulsion interfaces, improving the efficiency of the interfacial filter. Increasing the height of the emulsion reservoir would also be an easy way to increase contact between the two phases. Additionally, using a higher viscosity oil would address concerns for the potential volatility of the low viscosity oil and again improve trapping by increasing the time available for materials to diffuse to the emulsion interfaces.

While we have demonstrated our ability to trap proteins, there are many other materials which are known to collect at heterogeneous interfaces including algae, bacteria and other cells, medically relevant materials such as cholesterol and caffeine, polymers, surfactants, hydrocarbon materials such as phenols. While we have only performed a proof of concept for the emulsion interfacial filter with proteins, there is clear applicability to many industries including the medical professions and homeland security.

7. REFERENCES

1. Tupy, M. J., H.W. Blanch and C.J. Radke. "Total internal reflection fluorescence spectrometer to study dynamic adsorption phenomena at liquid/liquid interfaces." *Ind. Eng. Chem. Res.* **v37** (1998) 3159-3168.
2. Axelrod, D. , T.P. Burghardt and N.L. Thompson. "Total internal reflection fluorescence." *Ann. Rev. Biophys Bioeng.* **v13** (1984) 247-268.
3. Shashikala A.R. and A.M. Raichur. "Role of interfacial phenomena in determining adsorption of *Bacillus polymyxa* onto hematite and quartz." *Colloids and Surf. B* **v24(1)** (2002) 11-20.
4. Lukasik, J., T.M. Scott, D. Andryshak and S.R. Farrah. "Influence of salts on virus adsorption to microporous filters." *Appl. Environmental Microbiology* **v66(7)** (2000) 2914-2920.
5. Mukherjee, S., X. Zha, I. Tabas and F.R. Maxfield. "Cholesterol distribution in living cells: Fluorescence imaging using dehydroergosterol as a fluorescent analog." *Biophys. J.* **v75** (1998) 1915-1925.
6. Wang, Z., Z.Q. Shi, R.F. Shi and Y. Fan. "Studies on caffeine adsorption properties of phenolic resin adsorbent." *Acta Polymerica Sinica* #2 (4/2003) 211-215
7. Xu, X., V.T. John, G.L. McPherson, D.A. Grimm, J.A. Akkara and D. L. Kaplan. "A combined chemical-enzymatic method to remove selected aromatics from aqueous streams." *Appl. Biochem. Biotech.* **v51/52** (1995) 649-660.
8. Howse, J.R., R. Steitz, M. Pannek, P. Simon, D.W. Schubert and G. H. Findenegg. "Adsorbed surfactant layers at polymer/liquid interfaces. A neutron reflectivity study." *Phys Chem. Chem. Phys.* **v3(18)** (2001) 4044-4051.
9. Naumann, C.A., C.F. Brooks, G.G. Fuller, W. Knoll and C.W. Frank. "Viscoelastic properties of lipopolymers at the air-water interface: A combined interfacial stress rheometer and film balance study." *Langmuir* **v15** (1999) 7752.
10. Cai, J. and J.M. Prausnitz. "Density distribution for a polymer adsorbed at an oil-water interface." *J. Chem Phys.* **v117(8)** (2002) 3935.
11. Sensfelder, E., J. Burke and H.J. Ache. "Determination of hydrocarbons in water by evanescent wave absorption spectroscopy in the near-infrared region" *Fresenius' J. Anal. Chem.* **v354** (1996) 848-851.
12. Michalske, T. "Basic Research Needs for Countering Terrorism." presentation at the BES Workshop on Basic Research Needs to Counter Terrorism in Washington, DC (2002).
13. Lapidco-Encinas, B.H., B.A. Simmons, E.B. Cummings and Y. Fintschenko. "Dielectrophoretic concentration and separation of live and dead bacteria in an array of insulators." *Anal. Chem.* **v76(6)** (2004) 1571-1579.
14. Astorga-Wells, J. and H. Swerdlow. "Fluidic preconcentrator device for capillary electrophoresis of proteins." *Anal. Chem.* **v75(19)** (2003) 5207-5212.
15. Yang, H and R-L. Chien. "Sample stacking in laboratory on a chip devices." *J. Chromatogr. A* **v924** (2001) 155-163.
16. Huang, Z and C.F. Ivory. "Digitally controlled isoelectric focusing." *Anal. Chem.* **v71(8)** (1999) 1628-1632.
17. Khandurina, J., T.E. McKnight, S.C. Jacobson, L.C. Waters, R.S. Foote and J.M. Ramsey. "Integrated system for rapid PCR-based DNA analysis in microfluidic devices." *Anal. Chem.* **v72(13)** (2000) 2995-3000.

18. Vegvari, A. and S. Hjerten. "Hybrid microdevice electrophoresis of peptides, proteins, DNA, viruses and bacteria in various separation media using UV detection." *Electrophoresis* **v24** (2003) 3815-3820.
19. Williams, SKR and G.E. Kassalainen. "Lowering the molecular mass limit of thermal field-flow fractionation for polymer separations" *J. Chromatogr. A* **v988** (2003) 285-295.
20. Ross, D. and L.E. Locascio. "Microfluidic temperature gradient focusing." *Anal. Chem.* **v74(11)** (2002) 2556-2564.
21. Breadmore M.C., P.R. Haddad. "Approaches to enhancing the sensitivity of capillary electrophoresis methods for the determination inorganic and small organic anions." *Electrophoresis* **v22** (2001) 2464-2489.
22. Zhang, Y. and A.T. Timperman. "Integration of nano-capillary arrays into microfluidic devices for use as analyte concentrators." *Analyst* **v128** (2003) 537-542.
23. Xu, X.-J., P.-Y. Chow, C.-H. Quek, H.-H. Hng and L.-M. Gan. "Nanoparticles of polystyrene latexes by semicontinuous microemulsion polymerization using mixed surfactants." *J. Nanosci. Nanotech.* **v3(3)** (2003) 235-240.
24. http://en.wikipedia.org/wiki/Serum_albumin
25. http://en.wikipedia.org/wiki/Coal_bed_methane_extraction
26. Hightower, M.M., M.D. Siegel, J.M. Phelan, C.V. Williams, M.J. Kelley, W.-C. Cheng, Y. McClellan, G.S. Brown, S.L. Maffitt. "Innovative treatment & remediation demonstration program : FY 2000 year end report." SAND2001-1238P.
27. Adamson, A.W. and A.P. Gast *Physical Chemistry of Surfaces* 1997 John Wiley & Sons, New York, NY.
28. Friedenber, M.C., G.G. Fuller, C.W. Frank and C.R. Robertson. "Direct visualization of flow-induced anisotropy in a fatty acid monolayer." *Langmuir* **v12** (1996) 1594-1599.
29. Svitova, T.F., M.J. Wetherbee and C.J. Radke. "Dynamics of surfactant sorption at the air water interface: continuous-flow tensiometry." *J. Colloid Interface Sci.* **v261** (2003) 170-179.
30. Freer, E.M., K.S.Yim, G.G. Fuller and C.J. Radke. "Shear and dilatational relaxation mechanisms of globular and flexible proteins at the hexadecane/water interface." *Langmuir* **v20** (2004) 10159-10167.

APPENDIX A: CHEMICAL ANALYSIS OF COAL BED METHANE PRODUCED WATER

SANDIA NATIONAL LABORATORIES
attn: ALLAN R. SATTLER
PO BOX 5800 (MS-0706)
ALBUQUERQUE NM 87185

Explanation of codes	
B	Analyte Detected in Method Blank
E	Result is Estimated
H	Analyzed Out of Hold Time
N	Tentatively Identified Compound
S	Subcontracted
1-9	See Footnote

STANDARD

Assagai Analytical Laboratories, Inc.

Certificate of Analysis

All samples are reported on an "as received" basis, unless otherwise noted (e.g., Dry Weight).

Client: SANDIA NATIONAL LABORATORIES

Project:

Order: 0606256 SAN01 Receipt: 06-12-06

William P. Blava: President of Assagai Analytical Laboratories, Inc.

Sample: SAN JUAN METHANE WELL

Collected: 06-12-06 8:30:00 By: EDW

Matrix:

QC Group	Run Sequence	CAS #	Analyte	Result	Units	Dilution Factor	Detection Limit	Code	Prep Date	Run Date
0606256-0001A		SW846 5030B/8260B	Purgeable VOCs by GC/MS					By: TRS		
V06201	XG.2006.774.9	71-43-2	Benzene	ND	ug/L	1	1		06-13-06	06-13-06
V06201	XG.2006.774.9	100-41-4	Ethylbenzene	ND	ug/L	1	1		06-13-06	06-13-06
V06201	XG.2006.774.9	95-47-6	o-Xylene	ND	ug/L	1	1		06-13-06	06-13-06
V06201	XG.2006.774.9	106-38-3/106-42	p/m-Xylenes	ND	ug/L	1	2		06-13-06	06-13-06
V06201	XG.2006.774.9	106-86-3	Toluene	ND	ug/L	1	1		06-13-06	06-13-06
0606256-0001B		SW846 5030A/8015B	GRO by GC/FID					By: EJB		
V06204	XG.2006.776.5		Gasoline Range Organics	ND	mg/L	1	0.25		06-15-06	06-15-06
0606256-0001B		SW846 8015B	Diesel Range Organics by GC/FID					By: SDW		
S06333	XG.2006.791.6		Diesel Range Organics	ND	mg/L	1	25		06-19-06	06-23-06
0606256-0001C		SM 5310B/9060						By: CMC		
HEAL0606212	SB.2006.239.3	10-35-5	Carbon, Total Organic, TOC	ND	mg/L	10	10	S	06-19-06	06-19-06
0606256-0001D		SM 4500-P-B,D						By: MJN		
W06451	WC.2006.1477.14		Phosphorous, Total as P	0.89	mg/L	1	0.02		06-16-06	06-16-06
0606256-0001E		EPA 4.1.1/200.7 ICP						By: TGA		
M06606	MT.2006.1080.20	7440-21-3	Silica, dissolved	14.4	mg/L	11	0.5		06-13-06	06-16-06
0606256-0001F		EPA 120.1 Specific Conductance						By: MJN		
W00ND-06-082	WC.2006.1487.11	10-34-4	Conductivity	17540	umhos/cm	1	1		06-19-06	06-19-06
0606256-0001F		EPA 150.1 pH, Electrometric						By: NUL		
WPH06087	WC.2006.1495.1	10-29-7	pH	8.05	units	1	0.1		06-13-06	06-13-06
WPH06087	WC.2006.1495.1		sample temperature @	15.7	deg C	1	0		06-13-06	06-13-06

Page 1 of 2

Report Date: 6/29/2006 3:47:53 PM

Assaiel Analytical Laboratories, Inc.

Certificate of Analysis

All samples are reported on an "as received" basis, unless otherwise noted (i.e. - Dry Weight).

Client: SANDIA NATIONAL LABORATORIES

Project:

Order: 0606256 SAN01 Receipt: 06-12-06

Sample: SAN JUAN METHANE WELL

Collected: 06-12-06 9:30:00 By: EDW

Matrix:

QC Group	Run Sequence	CAS #	Analyte	Result	Units	Dilution Factor	Detection Limit	Code	Prep Date	Run Date
0606256-0001F			EPA 160.1 Total Dissolved Solids					By: MJN		
WTDS-06-064	WC.2006.1460.6	10-33-3	Total Dissolved Solids	11210	mg/L	1	10		06-14-06	06-15-06
0606256-0001F			EPA 300.0 Anions by IC					By: JTK		
W06443	WC.2006.1451.31	16887-00-6	Chloride	2060	mg/L	500	0.05		06-13-06	06-14-06
W06443	WC.2006.1451.14	14265-44-2	Orthophosphate, as P	0.330	mg/L	5	0.05		06-13-06	06-13-06
W06443	WC.2006.1451.14	14808-70-6	Sulfate	1.30	mg/L	5	0.05		06-13-06	06-13-06
0606256-0001F			EPA 310.1 Alkalinity, Titrimetric					By: NJL		
WALK06027	WC.2006.1490.22	71-52-3	Alkalinity, Bicarbonate	8550	mg/L	1	2		06-19-06	06-19-06
WALK06027	WC.2006.1490.22	3812-32-6	Alkalinity, Carbonate	ND	mg/L	1	2		06-19-06	06-19-06
WALK06027	WC.2006.1490.22	T-005	Alkalinity, Total	8550	mg/L	1	2		06-19-06	06-19-06
0606256-0001G			EPA 4.1.3/200.7 ICP					By: TGA		
MC6623	MT.2006.1102.33	7440-70-2	Calcium	22.5	mg/L	1	0.5		06-20-06	06-20-06
MC6623	MT.2006.1102.33	7439-89-6	Iron	ND	mg/L	1	0.5		06-20-06	06-20-06
MC6623	MT.2006.1102.33	7439-95-4	Magnesium	17.7	mg/L	1	0.5		06-20-06	06-20-06
MC6623	MT.2006.1102.33	7440-09-7	Potassium	39.2	mg/L	1	0.5		06-20-06	06-20-06
MC6623	MT.2006.1140.39	7440-23-5	Sodium	6100	mg/L	100	0.5		06-20-06	06-25-06
0606256-0001G			SM 2340B					By: DMS		
HARD	MT.2006.1155.1		Hardness, as CaCO ₃	129	mg/L	1	0		06-28-06	06-28-06
0606256-0001H			EPA 1654 - Solid Phase Extraction					By: NJL		
ORG06032	WC.2006.1450.9	10-30-0	Oil & Grease	ND	mg/L	1	5		06-13-06	06-13-06
0606256-0001I			EPA 418.1 Total Recoverable Petroleum Hydrocarbons					By: PW		
S06346	WC.2006.1539.4	10-90-2	TRPH	ND	mg/L	1	1		06-23-06	06-26-06

Unless otherwise noted, all samples were received in acceptable condition and all sampling was performed by client or client representative. Sample result of ND indicates Not Detected, i.e. result is less than the sample specific Detection Limit. Sample specific Detection Limit is determined by multiplying the sample Dilution Factor by the listed Reporting Detection Limit. All results relate only to the items tested. Any miscellaneous workorder information or footnotes will appear below.

Analytical results are not corrected for method blank or field blank contamination.

DISTRIBUTION

1	MS0521	Dick Damerow	02720
1	MS0706	Allan Sattler	06312
1	MS0734	Joel Hartenberger	01512
1	MS0734	Bruce Kelley	06334
1	MS0734	Margaret Welk	06338
1	MS0754	Emily Wright	06316
1	MS0755	Mike Hightower	06332
1	MS0824	Wahid Hermina	01510
1	MS0825	Carl Peterson	00003
1	MS0826	Dan Rader	01513
1	MS0834	Chris Bourdon	01513
1	MS0834	Carlton Brooks	01512
1	MS0834	Anne Grillet	01513
1	MS0834	Lisa Mondy	01514
1	MS0834	Tim O'Hern	01512
1	MS0834	Rob Tachau	01512
1	MS0834	Steven Trujillo	01512
1	MS0836	Richard Griffith	01517
1	MS0836	Andy Kraynik	01514
1	MS0836	Joel Lash	01514
1	MS1245	John Emerson	02453
2	MS9018	Central Technical Files	8944
2	MS0899	Technical Library	4536
1	MS0123	D. Chavez, LDRD Office	1011